

NUMERICAL METHODS

Conservative Scheme for the Thermodiffusion Stefan Problem

O. S. Mazhorova, Yu. P. Popov, and O. V. Shcheritsa

*Keldysh Institute of Applied Mathematics, Russian Academy of Sciences,
Moscow, Russia*

Received April 4, 2013

Abstract—We suggest further development of the principle of conservation for problems with moving boundaries. Using the problem of phase transitions in binary compounds as an example, we demonstrate a technique for constructing divergence and nondivergence finite difference schemes guaranteeing that the energy and mass conservation laws hold in the discrete model. In a class of front tracking methods, we prove the equivalence of the approach based on the use of moving grids with that based on a dynamic change of variables which permits one to solve the problem on a fixed grid.

DOI: 10.1134/S0012266113070094

1. INTRODUCTION

Studying physical processes by a finite difference method implies replacing a continuous medium by a discrete counterpart. This replacement can be performed in various ways, and for the original differential problem, there exists an unlimited variety of finite difference schemes. In this connection, one faces the problem of choosing a scheme with desired properties. The consistency, stability, and convergence conditions play a key role when assessing the performance of a numerical algorithm. These fundamental notions are of asymptotic nature. For sufficiently smooth solutions, these conditions involve the assumption that the grid increments tend to zero. For linear problems, the consistency and stability of a scheme imply its convergence.

However, numerical analysis of real-world problems often necessitates constructing finite difference schemes for nonlinear differential equations with discontinuous coefficients and solutions. As a rule, convergence analysis in such cases is restricted to making two (at best, three) computations on condensing grids, which requires an essential computational expenditures in multidimensional nonstationary problems. Moreover, the results of such computations do not in general provide reliable information on how well the discrete model describes the process to be studied [1, 2]. When numerically solving specific physical problems, an assessment of the performance of finite difference algorithms requires using additional considerations as well as the usual approximation, convergence, and stability requirements. One such performance criterion that should be used in the choice of a finite difference algorithm is given by the scheme principle of conservation, which follows from the physical meaning of the original problem.

The original physical-mathematical statement of the problem is the set of conservation laws determining the process in question. For example, in gas dynamics, these are the mass, momentum, and total energy conservation laws; in magnetic gas dynamics, they are supplemented with the magnetic flux conservation law. The principle of conservation says that the finite difference counterparts of these conservation laws should hold in a discrete model of a medium. The efficiency of the principle of conservation was illustrated for the first time by Tikhonov and Samarskii [2] who showed that conservation is a necessary condition for convergence in the case of a stationary heat equation with a discontinuous coefficient.

The subsequent development of the principle of conservation has led to the notion of total conservation [3, p. 360]. Totally conservative finite difference schemes form a subclass of the class of

conservative schemes. Not only the conservation laws themselves but also some of their corollaries hold in such schemes, including the first principle of thermodynamics in gas dynamics, balance for individual types of energy, and so on. The principles of conservation and total conservation are of physical origin and ensure that a finite difference model inherits the properties of the original physical-mathematical model. If these principles fail, then the corresponding discrete model becomes physically meaningless, and the solution of the finite difference problem differs quantitatively and sometimes even qualitatively from the true solution.

From the formal viewpoint, the total conservation property amounts to the following. The differential equations describing the original physical-mathematical model can be represented in various forms, which can be reduced to each other by equivalence transformations. For example, in gas dynamics, the divergence form of the energy equation expresses the conservation law for the total energy, and the nondivergence forms following from it express the first principle of thermodynamics and the balance of individual forms of energy. Total conservation means that the various representations of conservation laws in the discrete medium can be reduced to each other with the use of equivalence transformations similar to those in the differential case.

The present paper deals with some new aspects in the application of the principle of conservation to the solution of evolution problems in domains with moving boundaries for the case in which the law of their motion is not given in advance and should be determined in the course of the solution of the problem. For clarity, our exposition is based on an example of a problem on the crystallization of a solution whose phase transition temperature depends on the composition of the liquid and solid phases; this problem is known as the thermodiffusion Stefan problem. Although the principle of conservation has long become commonplace in the theory and practice of the construction and application of finite difference algorithms in numerical gas dynamics, the necessity to ensure that the conservation laws are satisfied in discrete models when numerically solving problems with phase transitions has only been recognized quite recently in connection with the analysis of phase transitions in multicomponent media [4]; moreover publications ignoring this principle [5–8] still continue to appear.

Of the broad variety of algorithms presently used for the numerical solution of phase transition problems (e.g., see [9, p. 163; 10, p. 343]), the present paper only considers methods in which the phase interface is explicitly singled out. They play an important role in the numerical analysis of phase transitions in multicomponent problems, where the temperature and composition on the solid–liquid interface is determined by the phase diagram of the system, the mass conservation law for each component, and the internal energy balance. The possibilities of using shock-capturing algorithms, which employ coefficient smoothing [11; 12, p. 274], or enthalpy methods [9, p. 217] for such problems are quite restricted.

In methods where the phase interface is singled out explicitly, the moving boundary is determined by the position of grid points fixed to it. This is achieved either by the use of moving grids coordinated in the original variables with the shape of the crystallization front [5, 6, 13–15] or by a dynamical change of variables [4; 10, p. 343; 16–20] that is chosen in such a way that the design domain in the new coordinates is regular and has fixed boundaries coinciding with coordinate lines (the front rectification method) [21]. The approximation is carried out for the original differential equations in the first case and for the equations obtained by the change of variables in the second case. Both approaches have their own advantages and disadvantages; the solution of the problem in the original coordinate system appears to be more “physical” than the use of a special coordinate system depending on the solution. The two approaches are equivalent as long as the statement of the differential problem is concerned.

In the present paper, for the thermodiffusion Stefan problem on a moving and a fixed grid, we construct divergence and nondivergence finite difference schemes ensuring the internal energy and mass balance. Just as the differential equations, the finite difference equations obtained in the framework of these two approaches can be reduced to each other by a change of variables.

2. THERMODIFFUSION STEFAN PROBLEM

Consider the problem on the crystallization of the binary compound $\mathcal{A}_x\mathcal{B}_{1-x}$ from the solution of the component \mathcal{A} in the substance \mathcal{B} , where x is the molar fraction. Suppose that the phase

transition occurs in a quasiequilibrium mode [22, p. 30]. This implies that the composition of both phases on the liquid–solid interface satisfies the phase diagram of the system: the liquid phase is a saturated solution with concentration $C^l = F_l(T)$ of the solute given by the liquidus line of the phase diagram, and the solid phase has the composition that is in equilibrium with the liquid phase and is given by the solidus line $C^s = F_s(C^l, T)$; here C^l and C^s are the volume concentrations of the component \mathcal{A} on the interface in the liquid and solid phases, respectively, and T is temperature. Here, unlike the classical Stefan problem, the phase transition temperature is not constant and depends on the liquid phase composition C^l and the solid phase composition C^s on the interface, $C^l \neq C^s$.

In the one-dimensional approximation, the distribution of temperature T and volume concentration C in the system is described by the system of equations

$$c_p^s \frac{\partial T}{\partial t} = \varkappa^s \frac{\partial^2 T}{\partial x^2}, \quad \frac{\partial C}{\partial t} = D^s \frac{\partial^2 C}{\partial x^2}, \quad 0 \leq x < \xi(t), \tag{1}$$

$$c_p^l \frac{\partial T}{\partial t} = \varkappa^l \frac{\partial^2 T}{\partial x^2}, \quad \frac{\partial C}{\partial t} = D^l \frac{\partial^2 C}{\partial x^2}, \quad \xi(t) \leq x < L. \tag{2}$$

Here x is the Cartesian coordinate, t is time, $\xi(t)$ is the interface position, and L is the domain length. The subdomain $0 \leq x < \xi(t)$ corresponds to the solid phase, and $\xi(t) < x \leq L$ to the liquid phase; c_p^l is the specific heat capacity, $\varkappa^s = k^s/\rho$, and $\varkappa^l = k^l/\rho$; k^s and k^l are the thermal conductivities, and D^s and D^l are the diffusion coefficient in the solid and liquid phases, respectively; ρ is the density. We assume that the liquid and solid phases have the same density.

The phase equilibrium conditions

$$C^l = F_l(T), \quad C^s = F_s(C^l, T), \tag{3}$$

the Stefan condition

$$\varkappa^s \frac{\partial T}{\partial x} \Big|_{x=\xi(t)-} - \varkappa^l \frac{\partial T}{\partial x} \Big|_{x=\xi(t)+} = \lambda \frac{d\xi}{dt}, \tag{4}$$

and the mass conservation law

$$D^s \frac{\partial C}{\partial x} \Big|_{x=\xi(t)-} - D^l \frac{\partial C}{\partial x} \Big|_{x=\xi(t)+} = -(C^s - C^l) \frac{d\xi}{dt} \tag{5}$$

hold on the interface; here λ is the latent heat of melting, and $d\xi/dt$ is the front velocity.

On the boundary of the domain, we pose the mass and heat no-flux conditions

$$\varkappa^s \frac{\partial T}{\partial x} = 0, \quad x = 0, \quad \varkappa^l \frac{\partial T}{\partial x} = 0, \quad x = L, \tag{6}$$

$$D^s \frac{\partial C^s}{\partial x} = 0, \quad x = 0, \quad D^l \frac{\partial C^l}{\partial x} = 0, \quad x = L. \tag{7}$$

We start the construction of finite difference schemes for the thermodiffusion Stefan problem by approximating Eqs. (1) and (2) represented in a coordinate system in which the interface is immovable.

3. FRONT RECTIFICATION METHOD

3.1. Change of Variables

In problem (1)–(7), we make a change of the independent variables (x, t) such that the position of the phase interface in the new coordinate system (y, t) is fixed and coincides with the point $y = 1$, and the boundary points $x = 0$ and $x = L$ of the domain becomes the points $y = 0$ and $y = 2$, respectively [21]. The old coordinates (x, t) and the new coordinates (y, t) is related by the formulas

$$t = t, \quad x = \varphi(y, t) = \begin{cases} y\xi(t) & \text{for } y \in [0, 1] \text{ in the solid phase,} \\ \xi(t) + (L - \xi(t))(y - 1) & \text{for } y \in [1, 2] \text{ in the liquid phase.} \end{cases} \tag{8}$$

The Jacobian J of this transformation is given by $J = \frac{(y, t)}{(x, \mathbf{t})} = \frac{1}{l}$, where $l = l(t)$ is the length of the corresponding zone in the original coordinate system; $l = l^s = \xi(\mathbf{t})$ in the solid phase, and $l = l^l = L - \xi(\mathbf{t})$ in the liquid phase. In the new variables, the domains $0 \leq y < 1$ and $1 < y \leq 2$ are filled with the solid and liquid phases, respectively.

Let us rewrite problem (1)–(7) in the variables (y, t) . One can readily see that

$$\frac{\partial}{\partial x} = \frac{1}{l} \frac{\partial}{\partial y}, \quad \frac{\partial}{\partial \mathbf{t}} = \frac{\partial}{\partial t} - \frac{\varphi_{\mathbf{t}}}{l} \frac{\partial}{\partial y}, \quad (9)$$

$$\varphi_{\mathbf{t}} = \begin{cases} y \frac{d\xi}{dt} & \text{for } y \in [0, 1], \\ (2 - y) \frac{d\xi}{dt} & \text{for } y \in [1, 2]. \end{cases} \quad (10)$$

The function $\varphi_{\mathbf{t}}$ is continuous at the point $y = 1$, and $\varphi_{\mathbf{t}}(1, \mathbf{t}) = d\xi/dt$.

Let us substitute the expressions (9) and (10) into the equation for the temperature,

$$c \left[\frac{\partial T}{\partial t} - \frac{\varphi_{\mathbf{t}}}{l} \frac{\partial T}{\partial y} \right] = \frac{1}{l} \frac{\partial}{\partial y} \left(\frac{\varkappa}{l} \frac{\partial T}{\partial y} \right), \quad y \in (0, 1) \cup (1, 2). \quad (11)$$

Here c , l , and \varkappa are piecewise constant functions taking the values c_p^s , l^s , and \varkappa^s for $y \in [0, 1)$ and c_p^l , l^l , and \varkappa^l for $y \in (1, 2]$.

At the point $y = 1$, we pose the Stefan condition

$$\left(\frac{\varkappa}{l} \frac{\partial T}{\partial y} \right) \Big|_{y=1-0} - \left(\frac{\varkappa}{l} \frac{\partial T}{\partial y} \right) \Big|_{y=1+0} = \lambda \frac{d\xi}{dt}. \quad (12)$$

We multiply Eq. (11) by the Jacobian of the transformation and write out the resulting equation in the divergence form

$$c \left[\frac{\partial}{\partial t} (lT) - \frac{\partial}{\partial y} (\varphi_{\mathbf{t}} T) \right] = \frac{\partial}{\partial y} \left(\frac{\varkappa}{l} \frac{\partial T}{\partial y} \right), \quad y \in (0, 1) \cup (1, 2). \quad (13)$$

When passing from Eq. (11) to (13), we have used the relation $\varphi_{\mathbf{t}y} = dl/dt$.

The equations for the concentration in the variables (y, t) in nondivergence and divergence forms read

$$l \frac{\partial C}{\partial t} - \varphi_{\mathbf{t}} \frac{\partial C}{\partial y} = \frac{\partial}{\partial y} \left(\frac{D}{l} \frac{\partial C}{\partial y} \right), \quad (14)$$

$$\frac{\partial}{\partial t} (lC) - \frac{\partial}{\partial y} (\varphi_{\mathbf{t}} C) = \frac{\partial}{\partial y} \left(\frac{D}{l} \frac{\partial C}{\partial y} \right), \quad y \in (0, 1) \cup (1, 2), \quad (15)$$

respectively. On the interface, we have

$$\left(\frac{D}{l} \frac{\partial C}{\partial y} \right) \Big|_{y=1-0} - \left(\frac{D}{l} \frac{\partial C}{\partial y} \right) \Big|_{y=1+0} = -(C^s - C^l) \frac{d\xi}{dt}. \quad (16)$$

Here $D = D^s$ for $y \in [0, 1)$ and $D = D^l$ for $y \in (1, 2]$.

To construct a finite difference algorithm, one can use both the divergence and nondivergence forms of the heat and mass balance equations; however, to obtain conservative schemes by the integro-interpolation method, it is convenient to use the equations represented in divergence form [23, p. 108].

3.2. Finite Difference Schemes and Grid Functions

In the domain $\mathcal{D}_y = [0, 2]$, we introduce the finite difference grid $\omega^y = \{y_i, 0 \leq i \leq N, y_0 = 0, y_N = 2\}$; then $h_{i+1/2} = y_{i+1} - y_i$ is the grid increment. Let the interface (the point $y = 1$) coincide with one of the grid points; we denote it by y_{i^*} . Along with the nodes y_i , we introduce the flow points $y_{i+1/2} = (y_i + y_{i+1})/2, i = 0, \dots, N - 1$, and the grid increments $\bar{h}_i^y = y_{i+1/2} - y_{i-1/2} = (h_{i+1/2}^y + h_{i-1/2}^y)/2$. The finite difference grid in time is denoted by $\omega^t = \{t_0 = 0, t_{j+1} = t_j + \tau, j = 0, 1, \dots\}$, where τ is the time grid increment.

In the space of the original variables, where the phase interface is moving, the nodes of the grid ω^y determine the points $\omega^x = \{x_i(t) = \varphi(y_i, t), 0 \leq i \leq N, x_0 = 0, x_N = L\}$. The node $x_{i^*}(t) = \varphi(y_{i^*}, t) = \xi(t)$ coincides with the phase interface,

$$h_{i+1/2}^x(t) = x_{i+1}(t) - x_i(t), \quad \bar{h}_i^x(t) = (h_{i+1/2}^x(t) + h_{i-1/2}^x(t))/2,$$

$$\widehat{h}_{i+1/2}^x = x_{i+1}(t + \tau) - x_i(t + \tau), \quad \widehat{\bar{h}}_i^x = (h_{i+1/2}^x(t + \tau) + h_{i-1/2}^x(t + \tau))/2.$$

The temperature and concentration grid functions are associated with grid nodes. Let $f = T, C$; then $f(x_i(t), t_j) = f(y_i, t_j) = f_i$. We define these functions on the intervals between the nodes as $f(x, t_j) = f(x_i(t), t_j)$ for $x \in (x_{i-1/2}, x_{i+1/2}), i \neq i^*$. On the interface, the temperature $T_{i^*-0} = T_{i^*+0}$ is continuous, and the concentration is discontinuous; therefore, two values of it, $C_{i^*-0} = C^s$ and $C_{i^*+0} = C^l$, are defined at the point i^* ; C^s and C^l are the equilibrium concentrations satisfying the phase diagram of the system; $C(x, t_j) = C_{i^*-0}$ if $x \in (x_{i^*-1/2}, x_{i^*})$, and $C(x, t_j) = C_{i^*+0}$ if $x \in (x_{i^*}, x_{i^*+1/2})$ (Fig. 1). To unify the notation, we also use C_{i-0} and $C_{i+0}, C_{i-0} = C_{i+0} = C_i$, at the regular points ($i \neq i^*$). The zone length, the specific heat capacity, the thermal diffusivity, and the diffusion coefficients refer to half-integer grid points. These functions are constant to the left and right of the point i^* and take the values corresponding to the solid and liquid phases, respectively.

We denote the finite difference time derivative by $f_{t,i} = f_t = (\widehat{f}_i - f_i)/\tau$, where

$$\widehat{f}_i = f(x_i(t + \tau), t_j + \tau) = f(y_i, t_j + \tau).$$

Let σ_α be a numerical parameter, $0 \leq \sigma_\alpha \leq 1$. By $f^{(\sigma_\alpha)} = \sigma_\alpha \widehat{f} + (1 - \sigma_\alpha)f$ we denote a linear combination of the values of a grid function on the upper and lower time layers; the passage from the weight σ_α to the weight σ_β is given by the formula $f^{(\sigma_\beta)} = f^{(\sigma_\alpha)} + (\sigma_\beta - \sigma_\alpha)\tau f_t$ [23, p. 17].

Let us define finite difference derivative operators with respect to space. On the fixed grid, we have

$$f_y = f_y(i) = \frac{f(y_{i+1}, t_j) - f(y_i, t_j)}{y_{i+1} - y_i}, \quad f_{\bar{y}}(i) = f_y(i - 1),$$

$$\widehat{f}_y = \widehat{f}_y(i) = \frac{f(y_{i+1}, t_j + \tau) - f(y_i, t_j + \tau)}{y_{i+1} - y_i}, \quad \widehat{f}_{\bar{y}}(i) = \widehat{f}_y(i - 1).$$

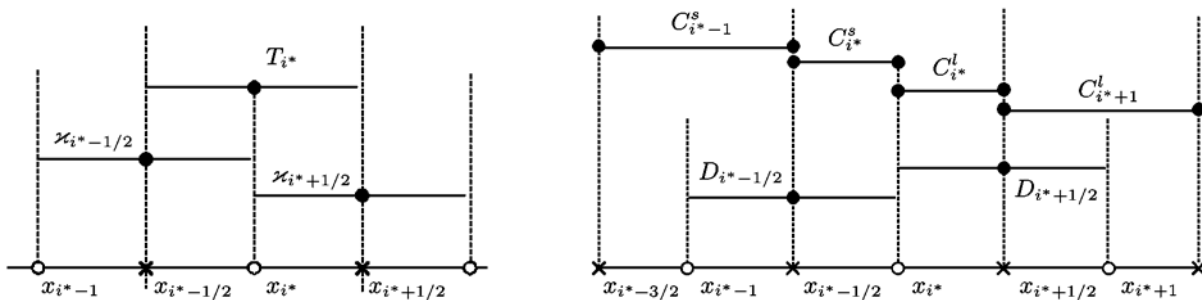


Fig. 1. Finite difference scheme. Grid functions.

In addition, let

$$f_{\bar{y}} = \frac{f(y_i) - f(y_{i-1/2})}{h_{i-1/2}^y/2}, \quad f_{\hat{y}} = \frac{f(y_{i+1/2}) - f(y_i)}{h_{i+1/2}^y/2}.$$

If $f(y_{i\pm 1/2}) = (f(y_{i\pm 1}) + f(y_i))/2$, then $f_{\bar{y}} = f_{\bar{y}}$ and $f_{\hat{y}} = f_{\hat{y}}$.

On the moving grid, we have

$$f_x = f_x(i) = \frac{f(x_{i+1}(\mathbf{t}_j), \mathbf{t}_j) - f(x_i(\mathbf{t}_j), \mathbf{t}_j)}{x_{i+1}(\mathbf{t}_j) - x_i(\mathbf{t}_j)}, \quad f_{\bar{x}}(i) = f_x(i-1),$$

$$\hat{f}_x = \hat{f}_x(i) = \frac{f(x_{i+1}(\mathbf{t}_j + \tau), \mathbf{t}_j + \tau) - f(x_i(\mathbf{t}_j + \tau), \mathbf{t}_j + \tau)}{x_{i+1}(\mathbf{t}_j + \tau) - x_i(\mathbf{t}_j + \tau)}, \quad \hat{f}_{\bar{x}}(i) = \hat{f}_x(i-1).$$

In what follows, we need finite difference differentiation formulas for the product,

$$(fg)_t = g^{(\sigma_\alpha)} f_t + f^{(1-\sigma_\alpha)} g_t, \quad (fg)_y = g f_y + f_{i+1} g_y.$$

3.3. Construction of a Finite Difference Scheme on a Fixed Grid

Let us integrate Eq. (13) over the grid cell $[y_{i-1/2}, y_{i+1/2}] \times [t_j, t_j + \tau]$,

$$\int_{t_j}^{t_j+\tau} \int_{y_{i-1/2}}^{y_{i+1/2}} \left[c \frac{\partial}{\partial t} (lT) - c \frac{\partial}{\partial y} (\varphi_t T) \right] dy dt = \int_{t_j}^{t_j+\tau} \int_{y_{i-1/2}}^{y_{i+1/2}} \frac{\partial}{\partial y} \left(\frac{\varkappa}{l} \frac{\partial T}{\partial y} \right) dy dt. \quad (17)$$

We substitute the grid functions into this relation and successively compute the integrals occurring in it. We obtain

$$\mathcal{I}_1 = \int_{t_j}^{t_j+\tau} dt \left[\int_{y_{i-1/2}}^{y_i} c_{i-1/2} \frac{\partial}{\partial t} (lT) dy + \int_{y_i}^{y_{i+1/2}} c_{i+1/2} \frac{\partial}{\partial t} (lT) dy \right]$$

$$= \frac{h_{i-1/2}^y}{2} c_{i-1/2} [(l_{i-1/2} T_i) - (l_{i-1/2} T_i)] + \frac{h_{i+1/2}^y}{2} c_{i+1/2} [(l_{i+1/2} T_i) - (l_{i+1/2} T_i)]. \quad (18)$$

If the integration interval $[y_{i-1/2}, y_{i+1/2}]$ does not contain the phase interface ($i \neq i^*$), then $c_{i-1/2} = c_{i+1/2}$, $l_{i-1/2} = l_{i+1/2}$, and the computation of the integral does not require splitting the integration domains into segments lying to the left and right from the point y_i ; however, the representation (18) provides a unified (independent of the node index) form of the finite difference approximation to the time derivative.

We split the integral of the second term on the left-hand side in relation (17) into two integrals and compute it with regard of the relations $(\varphi_t T)(y_i - 0) = (\varphi_t T)(y_i + 0)$ and $\varphi_t(y_{i^*}) = d\xi/dt$,

$$\mathcal{I}_2 = \int_{t_j}^{t_j+\tau} dt \left[\int_{y_{i-1/2}}^{y_i} c_{i-1/2} \frac{\partial}{\partial y} (\varphi_t T) dy + \int_{y_i}^{y_{i+1/2}} c_{i+1/2} \frac{\partial}{\partial y} (\varphi_t T) dy \right]$$

$$= \int_{t_j}^{t_j+\tau} [c_{i-1/2} [(\varphi_t T)(y_i) - (\varphi_t T)(y_{i-1/2})] + c_{i+1/2} [(\varphi_t T)(y_{i+1/2}) - (\varphi_t T)(y_i)]] dt$$

$$\approx \tau [(c_{i-1/2} - c_{i+1/2}) \xi_t T_{i^*}^{(\sigma_1)} + c_{i+1/2} (\varphi_t T^{(\sigma_1)})(y_{i+1/2}) - c_{i-1/2} (\varphi_t T^{(\sigma_1)})(y_{i-1/2})]. \quad (19)$$

Here $\xi_t = (\hat{\xi} - \xi)/\tau$ and $0 \leq \sigma_1 \leq 1$; we obtain an explicit approximation to the convective term for $\sigma_1 = 0$ and a purely implicit approximation for $\sigma_1 = 1$. Note that

$$\mathcal{I}_2 = \tau [c_{i+1/2} (\varphi_t T^{(\sigma_1)})(y_{i+1/2}) - c_{i-1/2} (\varphi_t T^{(\sigma_1)})(y_{i-1/2})]$$

at all grid nodes except for $i = i^*$. An additional term related to a jump in the thermodynamic parameters on the phase interface occurs only for $i = i^*$. The product $(\varphi_t T)$ at the half-integer points can be computed by the formula $(\varphi_t T)(y_{i\pm 1/2}) = \varphi_t(y_{i\pm 1/2})(T_i + T_{i\pm 1})/2$.

Let us proceed to the computation of the integral occurring on the right-hand side in relation (17),

$$\begin{aligned} \mathcal{I}_3 &= \int_{t_j}^{t_j+\tau} dt \left[\int_{y_{i-1/2}}^{y_i} \frac{\partial}{\partial y} \left(\frac{\varkappa}{l} \frac{\partial T}{\partial y} \right) dy + \int_{y_i}^{y_{i+1/2}} \frac{\partial}{\partial y} \left(\frac{\varkappa}{l} \frac{\partial T}{\partial y} \right) dy \right] \\ &= \int_{t_j}^{t_j+\tau} dt \left[\frac{\varkappa_{i-1/2}}{l_{i-1/2}} \frac{\partial T}{\partial y} \Big|_{y_{i-0}} - \frac{\varkappa_{i-1/2}}{l_{i-1/2}} \frac{\partial T}{\partial y} \Big|_{y_{i-1/2}} + \frac{\varkappa_{i+1/2}}{l_{i+1/2}} \frac{\partial T}{\partial y} \Big|_{y_{i+1/2}} - \frac{\varkappa_{i+1/2}}{l_{i+1/2}} \frac{\partial T}{\partial y} \Big|_{y_{i+0}} \right]. \end{aligned} \quad (20)$$

The heat flux is continuous at a regular point and experiences a jump, whose magnitude can be found from the Stefan condition (12), at the interface; therefore, we can write out an approximate expression for the integral \mathcal{I}_3 in the form

$$\mathcal{I}_3 \approx \tau \frac{d\xi}{dt} \lambda \delta_{ii^*} + \tau \left[\varkappa_{i+1/2} \left(\frac{T_y}{l_{i+1/2}} \right)^{(\sigma_2)} - \varkappa_{i-1/2} \left(\frac{T_{\bar{y}}}{l_{i-1/2}} \right)^{(\sigma_2)} \right], \quad (21)$$

where δ_{ii^*} is the Kronecker delta.

By replacing the integrals in (17) with their approximations (18), (19), and (21), we obtain a divergence finite difference scheme with weights σ_1 and σ_2 for Eqs. (13) and (12) multiplied by the cell area. After the division by τ , it acquires the form

$$\begin{aligned} &0.5h_{i-1/2}^y c_{i-1/2} (l_{i-1/2} T_i)_t + 0.5h_{i+1/2}^y c_{i+1/2} (l_{i+1/2} T_i)_t \\ &\quad - [c_{i+1/2} (\varphi_t T^{(\sigma_1)})(y_{i+1/2}) - c_{i-1/2} (\varphi_t T^{(\sigma_1)})(y_{i-1/2})] \\ &= \left[\varkappa_{i+1/2} \left(\frac{T_y}{l_{i+1/2}} \right)^{(\sigma_2)} - \varkappa_{i-1/2} \left(\frac{T_{\bar{y}}}{l_{i-1/2}} \right)^{(\sigma_2)} \right] + \xi_t \left[\lambda \delta_{ii^*} + (c_{i-1/2} - c_{i+1/2}) T_{i^*}^{(\sigma_1)} \right]. \end{aligned} \quad (22)$$

At a regular point, relation (22) is a scheme with central differences for an equation of convection-diffusion type. If $i = i^*$, then it is supplemented with a term due to a jump in the thermodynamic parameters on the interface and heat release (or absorption) during the phase transition.

To approximate the boundary conditions at the points y_0 and y_N , one should integrate Eq. (13) with regard of (6) over the intervals $[y_0, y_{1/2}]$ and $[y_{N-1/2}, y_N]$, respectively. As a result, we obtain

$$\begin{aligned} &0.5h_{1/2}^y c_{1/2} (l_{1/2} T_0)_t - c_{1/2} (\varphi_t T^{(\sigma_1)})(y_{1/2}) = \varkappa_{1/2} (T_y/l_{1/2})^{(\sigma_2)}, \\ &0.5h_{N-1/2}^y c_{N-1/2} (l_{N-1/2} T_N)_t + c_{N-1/2} (\varphi_t T^{(\sigma_1)})(y_{N-1/2}) = -\varkappa_{N-1/2} (T_{\bar{y}}/l_{N-1/2})^{(\sigma_2)}. \end{aligned} \quad (23)$$

The finite difference problem (22), (23) is nonlinear. Here the unknowns are the temperature \widehat{T}_i on the upper time layer and the interface velocity ξ_t . The lengths of the solid and liquid zones and φ_t can obviously be expressed via ξ_t . (For the unknown function one can take the length of some zone as well, and the front velocity can be computed on the basis of the change in the zone length in one time step.)

To construct a finite difference approximation to the diffusion equation, we integrate equation (15) over the cell $[y_{i-1/2}, y_{i+1/2}] \times [t_j, t_j + \tau]$,

$$\int_{t_j}^{t_j+\tau} \int_{y_{i-1/2}}^{y_{i+1/2}} \left[\frac{\partial}{\partial t} (lC) - \frac{\partial}{\partial y} (\varphi_t C) \right] dy dt = \int_{t_j}^{t_j+\tau} \int_{y_{i-1/2}}^{y_{i+1/2}} \frac{\partial}{\partial y} \left(\frac{D}{l} \frac{\partial C}{\partial y} \right) dy dt.$$

Just as above, we split the integral with respect to the space variable into two integrals. If the integration interval contains the interface, then, in addition to l and D , the concentration $C_{i^*-0} = C^s$, $C_{i^*+0} = C^l$, has a discontinuity at the point i^* . At the regular points, we have $C_{i-0} = C_{i+0}$. After simple transformations similar to (18)–(21), we obtain

$$\begin{aligned} & 0.5h_{i-1/2}^y[(\widehat{l_{i-1/2}C_{i-0}}) - (l_{i-1/2}C_{i-0})] + 0.5h_{i+1/2}^y[(\widehat{l_{i+1/2}C_{i+0}}) - (l_{i+1/2}C_{i+0})] \\ & \quad - \tau[(C^{s,(\sigma_3)} - C^{l,(\sigma_3)})\xi_t\delta_{ii^*} + (\varphi_t C^{(\sigma_3)})(y_{i+1/2}) - (\varphi_t C^{(\sigma_3)})(y_{i-1/2})] \\ & = \tau[D_{i+1/2}(C_y/l_{i+1/2})^{(\sigma_4)} - D_{i-1/2}(C_{\bar{y}}/l_{i-1/2})^{(\sigma_4)}] - \tau(C^{s,(\sigma_4)} - C^{l,(\sigma_4)})\xi_t\delta_{ii^*}. \end{aligned} \quad (24)$$

In the last integral on the right-hand side, we pass from the weight σ_4 to the weight σ_3 and collect similar terms containing ξ_t . After the division by τ , we rewrite Eq. (24) as follows:

$$\begin{aligned} & 0.5h_{i-1/2}^y[(\widehat{l_{i-1/2}C_{i-0}}) - (l_{i-1/2}C_{i-0})]/\tau + 0.5h_{i+1/2}^y[(\widehat{l_{i+1/2}C_{i+0}}) - (l_{i+1/2}C_{i+0})]/\tau \\ & \quad - (\varphi_t C^{(\sigma_3)})(y_{i+1/2}) - (\varphi_t C^{(\sigma_3)})(y_{i-1/2}) \\ & = D_{i+1/2}(C_y/l_{i+1/2})^{(\sigma_4)} - D_{i-1/2}(C_{\bar{y}}/l_{i-1/2})^{(\sigma_4)} + \tau(\sigma_3 - \sigma_4)(C_t^s - C_t^l)\xi_t\delta_{ii^*}. \end{aligned} \quad (25)$$

If $\sigma_3 = \sigma_4$, then the finite difference equation (25) is a natural approximation to the divergence form of the mass conservation law and is independent of the grid point number. If $\sigma_3 \neq \sigma_4$, then the conservative finite difference scheme contains the source/drain $\tau(\sigma_3 - \sigma_4)(C_t^s - C_t^l)\xi_t$ localized at the point $i = i^*$ and associated with a time-dependent jump in the concentration on the interface. In what follows, we consider the case in which $\sigma_3 = \sigma_4$.

We obtain an approximation to the boundary conditions (7) if we equate the terms with indices $0 - 1/2$ and $N + 1/2$ in (25) for $i = 0$ and $i = N$, respectively, with zero. This can readily be verified by integrating Eq. (15) over the cells adjacent to the boundary with regard of conditions (7).

3.4. Approximation to the Heat Transfer Equation in Nondivergence Form

The heat transfer and solute transport equations admit the divergence form (13), (15) and the nondivergence form (11), (14). In the construction of the finite difference schemes (22) and (25), we have used the divergence form of the corresponding equations. By analogy with the differential case, let us transform the constructed schemes into nondivergence form. We start from a grid equation for the temperature. Let us rewrite the scheme (22) in the form

$$\begin{aligned} & 0.5h_{i-1/2}^y c_{i-1/2} (l_{i-1/2} T_i)_t + 0.5h_{i+1/2}^y c_{i+1/2} (l_{i+1/2} T_i)_t \\ & \quad - [0.5h_{i-1/2}^y c_{i-1/2} (\varphi_t T^{(\sigma_1)})_{\bar{y}} + 0.5h_{i+1/2}^y c_{i+1/2} (\varphi_t T^{(\sigma_1)})_{\bar{y}}] \\ & = [\varkappa_{i+1/2} (T_y/l_{i+1/2})^{(\sigma_2)} - \varkappa_{i-1/2} (T_{\bar{y}}/l_{i-1/2})^{(\sigma_2)}] + \xi_t \lambda \delta_{ii^*} \end{aligned} \quad (26)$$

and use the finite difference differentiation formulas for the product,

$$\begin{aligned} & 0.5h_{i-1/2}^y c_{i-1/2} [l_{i-1/2}^{(\sigma_0)} T_{t,i} + T_i^{(1-\sigma_0)} l_{t,i-1/2}] + 0.5h_{i+1/2}^y c_{i+1/2} [l_{i+1/2}^{(\sigma_0)} T_{t,i} + T_i^{(1-\sigma_0)} l_{t,i+1/2}] \\ & \quad - [0.5h_{i-1/2}^y c_{i-1/2} (\varphi_t \tilde{y} T_i^{(\sigma_1)} + \varphi_{t,i-1/2} T_{\bar{y}}^{(\sigma_1)}) + 0.5h_{i+1/2}^y c_{i+1/2} (\varphi_{t\bar{y}} T_i^{(\sigma_1)} + \varphi_{t,i+1/2} T_{\bar{y}}^{(\sigma_1)})] \\ & = [\varkappa_{i+1/2} (T_y/l_{i+1/2})^{(\sigma_2)} - \varkappa_{i-1/2} (T_{\bar{y}}/l_{i-1/2})^{(\sigma_2)}] + \xi_t \lambda \delta_{ii^*}. \end{aligned} \quad (27)$$

Note that $h_{i-1/2}^y l_{t,i-1/2}/2 = (y_i - y_{i-1/2})l_{t,i-1/2} = y_i l_{t,i-0} - y_{i-1/2} l_{t,i-1/2} = h_{i-1/2}^y \varphi_{t\bar{y}}/2$, and likewise, $h_{i+1/2}^y l_{t,i+1/2}/2 = h_{i+1/2}^y \varphi_{t\bar{y}}/2$. We substitute these expressions into (27) and pass from the weight $1 - \sigma_0$ to the weight σ_1 . After matching like terms, Eq. (26) acquires the form

$$\begin{aligned} & 0.5h_{i-1/2}^y c_{i-1/2} l_{i-1/2}^{(\sigma_0)} T_{t,i} + 0.5h_{i+1/2}^y c_{i+1/2} l_{i+1/2}^{(\sigma_0)} T_{t,i} \\ & \quad - [0.5h_{i-1/2}^y c_{i-1/2} \varphi_{t,i-1/2} T_{\bar{y}}^{(\sigma_1)} + 0.5h_{i+1/2}^y c_{i+1/2} \varphi_{t,i+1/2} T_{\bar{y}}^{(\sigma_1)}] + Q_i^T \\ & = [\varkappa_{i+1/2} (T_y/l_{i+1/2})^{(\sigma_2)} - \varkappa_{i-1/2} (T_{\bar{y}}/l_{i-1/2})^{(\sigma_2)}] + \xi_t \lambda \delta_{ii^*}, \end{aligned} \quad (28)$$

where

$$Q_i^T = (1 - \sigma_0 - \sigma_1)\tau T_{t,i} [h_{i-1/2}^y c_{i-1/2} \varphi_{t\bar{y}} + ch_{i+1/2}^y c_{i+1/2} \varphi_{t\bar{y}}] / 2.$$

Equation (28) is algebraically equivalent to (22) and hence provides the correct heat balance in the discrete model as well.

By comparing Eq. (28) with (14), we find that, in addition to an approximation to the terms occurring in the nondivergence differential equation, the finite difference equation contains the extra term Q_i^T . It can be treated as a source that acts on each interval of the finite difference grid and counterbalances the heat imbalance due to an uncoordinated approximation to various terms of the differential equation in time. The relation $Q_i^T = 0$ holds for the coordinated choice of the time weights such that $\sigma_0 + \sigma_1 = 1$.

The transformation of the finite difference scheme (25) to nondivergence form leads to the scheme

$$\begin{aligned} &0.5h_{i-1/2}^y l_{i-1/2}^{(\sigma_5)} C_{t,i-0} + 0.5h_{i+1/2}^y l_{i+1/2}^{(\sigma_5)} C_{t,i+0} \\ &\quad - [0.5h_{i-1/2}^y \varphi_{t,i-1/2} C_{\bar{y}}^{(\sigma_3)} + 0.5h_{i+1/2}^y \varphi_{t,i+1/2} C_y^{(\sigma_3)}] + Q_i^C \\ &= [D_{i+1/2} (C_y / l_{i+1/2})^{(\sigma_3)} - D_{i-1/2} (C_{\bar{y}} / l_{i-1/2})^{(\sigma_3)}] + \xi_t (C_{i+0}^{(\sigma_3)} - C_{i-0}^{(\sigma_3)}) \delta_{ii^*}. \end{aligned} \tag{29}$$

Here

$$Q_i^C = (1 - \sigma_3 - \sigma_5)\tau [h_{i-1/2}^y \varphi_{t\bar{y}} C_{t,i-0} + h_{i+1/2}^y \varphi_{t\bar{y}} C_{t,i+0}] / 2$$

is a mass source (drain), whose occurrence, just as in the scheme (28), is due to the uncoordinated choice of the time weights in various terms of the finite difference equation. We have thereby proved the following assertion.

Assertion 1. *The finite difference schemes (22) and (28) approximating the nondivergence and divergence forms of the heat equation are algebraically equivalent.*

A similar assertion holds for the finite difference schemes (25) and (29), which approximate the nondivergence and divergence forms of the equation for the concentrations.

The conditions $\sigma_0 + \sigma_1 = 1$ and $\sigma_3 + \sigma_5 = 1$ single out the class of nondivergence finite difference schemes that ensure the conservation laws to hold without any correction terms. How essential the influence of the terms Q_i^T and Q_i^C is in the case where either $\sigma_0 + \sigma_1 \neq 1$ or $\sigma_3 + \sigma_5 \neq 1$ depends on the solution properties such as the interface motion velocity, the medium parameters, the phase diagram of the system, the finite difference grid, etc.

We also point out that the requirement that the divergence and nondivergence forms of the finite difference problem be equivalent determines how the spatial derivatives are approximated. For example, the frequently used representation of the term $\frac{\partial \varphi}{\partial t} \frac{\partial f}{\partial y}$, $f = T, C$, in the form $\varphi_{t,i} (f_y + \bar{f}_y) / 2$ (e.g., see [10, p. 347; 24; 25]) does not satisfy this requirement and results in a failure of the conservation laws in the system.

4. METHOD OF COMPUTATIONS ON THE MOVING GRID

4.1. Construction of the Finite Difference Scheme

Now let us use the integro-interpolation method to construct a finite difference approximation to Eqs. (1) and (2) on the grid $\omega_x \times \omega_t$. We integrate Eqs. (1) and (2) over the cell $[x_{i-1/2}(t), x_{i+1/2}(t)] \times [t_j, t_j + \tau]$,

$$\int_{t_j}^{t_j+\tau} \int_{x_{i-1/2}(t)}^{x_{i+1/2}(t)} c \frac{\partial}{\partial t} T dx dt = \int_{t_j}^{t_j+\tau} \int_{x_{i-1/2}(t)}^{x_{i+1/2}(t)} \frac{\partial}{\partial x} \left(\kappa \frac{\partial T}{\partial x} \right) dx dt, \tag{30}$$

and successively transform the integrals occurring on the left- and right-hand sides in relation (30). We split each of them into two integrals over closed intervals $[x_{i-1/2}(t), x_i(t)]$ and $[x_i(t), x_{i+1/2}(t)]$.

On the left-hand side, we use the differentiation formula for an integral with variable integration limits. As a result, we obtain

$$\begin{aligned} \mathcal{I}_1^x = & \int_{t_j}^{t_j+\tau} dt \frac{d}{dt} \int_{x_{i-1/2}(t)}^{x_i(t)} cT dx - \int_{t_j}^{t_j+\tau} dt \left[(cT)|_{x_i-0} \frac{dx_i}{dt} - (cT)|_{x_{i-1/2}} \frac{dx_{i-1/2}}{dt} \right] \\ & + \int_{t_j}^{t_j+\tau} dt \frac{d}{dt} \int_{x_i(t)}^{x_{i+1/2}(t)} cT dx - \int_{t_j}^{t_j+\tau} dt \left[(cT)|_{x_{i+1/2}} \frac{dx_{i+1/2}}{dt} - (cT)|_{x_i+0} \frac{dx_i}{dt} \right]. \end{aligned} \tag{31}$$

We substitute the values of the grid functions into relation (31) and write out an approximate expression for \mathcal{I}_1^x in the form

$$\begin{aligned} & 0.5c_{i-1/2}[(\widehat{h_{i-1/2}^x T_i}) - (h_{i-1/2}^x T_i)] + 0.5c_{i+1/2}[(\widehat{h_{i+1/2}^x T_i}) - (h_{i+1/2}^x T_i)] \\ & - \tau[(cT^{(\sigma_1)})_{i+1/2} x_{i+1/2,t} - (cT^{(\sigma_1)})_{i-1/2} x_{i-1/2,t}] - \tau[c_{i-1/2} - c_{i+1/2}] T_i^{(\sigma_1)} x_{i,t}, \end{aligned} \tag{32}$$

where $x_{i,t} = (\hat{x}_i - x_i)/\tau$. The last bracketed expression in (32) is only nonzero for $i = i^*$.

The approximation to the integral on the right-hand side in relation (30) is constructed just as in (20); one should only use the fact that, in this case, the space grid increment depends on time,

$$\mathcal{I}_2^x \simeq \tau[x_{it} \lambda \delta_{ii^*} + \varkappa_{i+1/2} T_x^{(\sigma_2)} - \varkappa_{i-1/2} T_{\bar{x}}^{(\sigma_2)}]. \tag{33}$$

By matching the expressions (32) and (33) obtained after the division by τ , we write out the finite difference scheme on the moving grid as follows:

$$\begin{aligned} & 0.5[c_{i-1/2}(h_{i-1/2}^x T_i)_t + c_{i+1/2}(h_{i+1/2}^x T_i)_t] - [(cT^{(\sigma_1)})_{i+1/2} x_{t,i+1/2} - (cT^{(\sigma_1)})_{i-1/2} x_{t,i-1/2}] \\ & = [\varkappa_{i+1/2} T_x^{(\sigma_2)} - \varkappa_{i-1/2} T_{\bar{x}}^{(\sigma_2)}] + \xi_t [\lambda \delta_{ii^*} + [c_{i-1/2} - c_{i+1/2}] T_i^{(\sigma_1)}]. \end{aligned} \tag{34}$$

The integration of the equation for the concentration over the cell $[x_{i-1/2}, x_{i+1/2}] \times [t_j, t_j + \tau]$ leads to the relation

$$\begin{aligned} & 0.5[(h_{i-1/2}^x C_{i-0})_t + (h_{i+1/2}^x C_{i+0})_t] - [C_{i+1/2}^{(\sigma_3)} x_{t,i+1/2} - C_{i-1/2}^{(\sigma_3)} x_{t,i-1/2}] \\ & = [D_{i+1/2} C_x^{(\sigma_3)} - D_{i-1/2} C_{\bar{x}}^{(\sigma_3)}]. \end{aligned} \tag{35}$$

The approximation at the points x_0 and x_N is constructed on the basis of integrals over the intervals $[0, x_{1/2}]$ and $[x_{N-1/2}, x_N]$.

The finite difference equations (34) and (35) also admit nondivergence form, which can be obtained just as in Subsection 3.4.

Assertion 2. *The families of finite difference schemes (22) and (34) constructed by the front rectification method and on a moving grid, respectively, are algebraically equivalent.*

Proof. The grid relations (22) and (34) approximate integral relations that pass into each other under the change of variables 3.1. One can readily see that, in the space of grid functions, the discrete counterpart of 3.1 provides the same relationship between the finite difference equations (34), (22) and (35), (25), respectively. Indeed,

$$\begin{aligned} h_{i+1/2}^x &= x_{i+1}(t) - x_i(t) = \varphi(y_{i+1}, t) - \varphi(y_i, t) = (y_{i+1} - y_i) l_{i+1/2}(t) = h_{i+1/2}^y l_{i+1/2}(t), \\ \widehat{h_{i+1/2}^x} &= h_{i+1/2}^y l_{i+1/2}(t + \tau), \quad x_{t,i\pm 1/2} = \varphi_t(y_{i\pm 1/2}, t). \end{aligned} \tag{36}$$

Let us substitute the expressions (36) into Eqs. (34) and (35) shifting the indices where necessary. As a result, we obtain the schemes (22) and (25). Therefore, the families of finite difference schemes

constructed with the use of the front rectification method and on a moving grid are algebraically equivalent. This is the case for nondivergence schemes as well. Just as in the differential case, one family can be reduced to another by a change of variables. The proof of Assertion 2 is complete. A similar assertion holds for the finite difference schemes (25) and (35).

4.2. Conservation Laws in the Discrete Model

Equations (1) and (2) and the Stefan conditions (3) and (4) are a consequence of the conservation law for the internal energy in a system with a phase transition. Let us show that the internal energy conservation law holds as well in the discrete model where the heat transfer is described by Eq. (34).

Assertion 3. *The finite difference counterpart of the internal energy conservation law holds for the finite difference scheme (34).*

Proof. Suppose that the phase transition occurs at a constant temperature $T_{i^*} = \text{const}$ and introduce the specific internal energy as follows:

$$\begin{aligned} \mathcal{E} &= \mathcal{E}^s = c^s T, & T < T_{i^*} & \text{ in the solid phase,} \\ \mathcal{E} &= \mathcal{E}^l = c^s T_{i^*} + c^l (T - T_{i^*}) + \lambda, & T > T_{i^*} & \text{ in the liquid phase.} \end{aligned} \tag{37}$$

First, we write out the internal energy balance on the interval $[x_{i^*-1/2}, x_{i^*+1/2}]$, which contains the interface. From (37), we have $c_{i-1/2} T_{i^*} = c^s T_{i^*} = \mathcal{E}_{i^*-0}$ and $c_{i+1/2} T_{i^*} = c^l T_{i^*} = \mathcal{E}_{i^*+0} + (c^l - c^s) T_{i^*} - \lambda$. We use these relations in Eq. (34) and make simple transformations; then we obtain the equation

$$0.5[\mathcal{E}^s h_{i^*-1/2}^x + \mathcal{E}^l h_{i^*+1/2}^x]_t = [\mathcal{E}_{i^*+1/2}^{l,(\sigma_1)} x_{t,i^*+1/2} - \mathcal{E}_{i^*-1/2}^{s,(\sigma_1)} x_{t,i^*-1/2}] + \varkappa_{i^*+1/2} T_x^{(\sigma_2)} - \varkappa_{i^*-1/2} T_{\bar{x}}^{(\sigma_2)},$$

where $\mathcal{E}_{i^*+1/2}^{l,(\sigma_1)} = (cT^{(\sigma_1)})_{i^*+1/2} + (c^s - c^l) T_{i^*} + \lambda$ and $\mathcal{E}_{i^*-1/2}^{s,(\sigma_1)} = (cT^{(\sigma_1)})_{i^*-1/2}$. This is the internal energy balance equation for the cell $[x_{i^*-1/2}, x_{i^*+1/2}]$. One can readily write out the energy balance for any interval $[x_{i-1/2}, x_{i+1/2}]$, $1 \leq i \leq N - 1$, without singling out the case of $i = i^*$,

$$0.5[\mathcal{E}_{i-0} h_{i-1/2}^x + \mathcal{E}_{i+0} h_{i+1/2}^x]_t = [\mathcal{E}_{i+1/2}^{(\sigma_1)} x_{t,i+1/2} - \mathcal{E}_{i-1/2}^{(\sigma_1)} x_{t,i-1/2}] + \varkappa_{i+1/2} T_x^{(\sigma_2)} - \varkappa_{i-1/2} T_{\bar{x}}^{(\sigma_2)}. \tag{38}$$

We have $\mathcal{E}_{i-0} = \mathcal{E}_{i+0}$ inside each zone and $\mathcal{E}_{i-0} = \mathcal{E}_{i^*}^s$ and $\mathcal{E}_{i+0} = \mathcal{E}_{i^*}^l$ on the interface. Since the heat flux at the points x_0 and x_N is zero, in the cells adjacent to the boundary, we have

$$0.5[\mathcal{E}_0 h_{1/2}^x]_t = \mathcal{E}_{1/2}^{(\sigma_1)} x_{t,1/2} + \varkappa_{i+1/2} T_x^{(\sigma_2)}, \quad 0.5[\mathcal{E}_N h_{N-1/2}^x]_t = -\mathcal{E}_{N-1/2}^{(\sigma_1)} x_{t,N-1/2} - \varkappa_{N-1/2} T_{\bar{x}}^{(\sigma_2)}. \tag{39}$$

The internal energy of this system is computed by the formula

$$E = \mathcal{E}_0 h_{1/2}^x + \sum_{i=1}^{N-1} [\mathcal{E}_{i-0} h_{i-1/2}^x + \mathcal{E}_{i+0} h_{i+1/2}^x] + \mathcal{E}_N h_{N-1/2}^x.$$

By summing relations (38) and (39) over all i , we obtain $E_t = 0$. The approximation to the original differential problem by the finite difference relations (38) and (39) ensures the conservation law for the internal energy in a discrete medium. The proof of Assertion 3 is complete.

The summation of Eq. (35) over all grid points justifies the mass conservation law. Here, just as above, the approximation to the conditions on the interface and the domain boundaries is coordinated with the approximation at the interior nodes.

Obviously, the internal energy and mass balance holds if equivalent nondivergence finite difference schemes are used instead of divergence schemes.

5. RESULTS OF COMPUTATIONS

Let us illustrate the properties of the constructed finite difference schemes by an example dealing with the problem on the crystallization of a binary compound in isothermal conditions from a supersaturated solution [22, p. 30].

Consider a binary composition whose phase diagram has the form

$$C^l(T) = \gamma(T - T^*) + \bar{C}, \quad C^s(T) = \bar{C}, \quad \gamma > 0. \tag{40}$$

At the initial time, at temperature $T = T_0$, the solid phase $C^s(T_0) = \bar{C}$ of the composition is put in contact with a solution supersaturated at that temperature. The composition of the liquid phase is $C_{\text{begin}} = C^l(T_0 + \delta T) > C^l(T_0)$, $\delta T > 0$, its length is l_0^l , the length of the solid phase is l_0^s , and the phase interface is at the point $\xi(0) = 0$. We assume that the system is in isothermal conditions, the heat absorption on the crystallization front can be neglected, and the solute does not enter the liquid phase from the outside. The crystallization process, which starts as a result of contact of the solid phase with the supersaturated liquid, continues until the composition of the entire liquid phase becomes homogeneous and equal to $C^l(T_0)$. By virtue of the mass conservation law, at the time of growth termination, the width of the grown crystal should be equal to

$$\Delta = l_0^l (C_{\text{begin}}^l - C^l(T_0)) / l(\bar{C} - C^l(T_0)).$$

Under these conditions, the crystallization process is described by an equation for the concentration with conditions (40) and (5) on the phase boundary and with condition (7) on the domain boundary at the points $x = -l_0^s$ and $x = l_0^l$.

We take $l_0^l = 1$, $l_0^s = 0.1$, $T_0 = 1700K$, and $\delta T = 10$ and set the composition of the solid phase to unity, $\bar{C} = 1$; the phase diagram parameters correspond to the data for CuFe [26], $\gamma = 0.06$ and $T^* = 1713.(3)K$. The solute concentration in the saturated solution at temperature T_0 is $C^l(T_0) = 0.2$, the initial composition of the liquid phase is $C_{\text{begin}} = 0.8$, $D^l = 5 \times 10^{-5}$, and the time scale is $t_D = (l_0^l)^2 / D^l$. For the chosen parameter values, we have $\Delta = 0.75$.

We solve the isothermal crystallization problem on a uniform fixed grid $\omega_y \times \omega_t$. The number of nodes is $i^* = 10$ in the solid phase and 500 in the liquid phase. We carry out the computations with the use of two nondivergence finite difference schemes obtained from the family (29).

One of them corresponds to the parameter values $\sigma_3 = 1$ and $\sigma_5 = 0$ (scheme I). In this case, we have $Q_i^C = 0$. Scheme I is algebraically equivalent to a divergence scheme in the family (25) and hence guarantees that the mass conservation law holds.

Scheme II is obtained from the family (29) for the parameter values $\sigma_3 = \sigma_5 = 1$, the corresponding value of Q_i^C is $-\tau[h_{i-1/2}^y \varphi_{t\bar{y}} C_{t,i-0} + h_{i+1/2}^y \times 2\varphi_{t\bar{y}} C_{t,i+0}] / 2$, and $Q_i^C = 0$ for $i < i^*$, because $C_{t,i\pm 0} = 0$ in the solid phase. In the liquid and on the interface, Q_i^C is nonzero; however, it was assumed in the computations that $Q_i^C \equiv 0$. This essentially implies that mass loss at the rate Q_i^C occurs in the liquid phase on each grid interval.

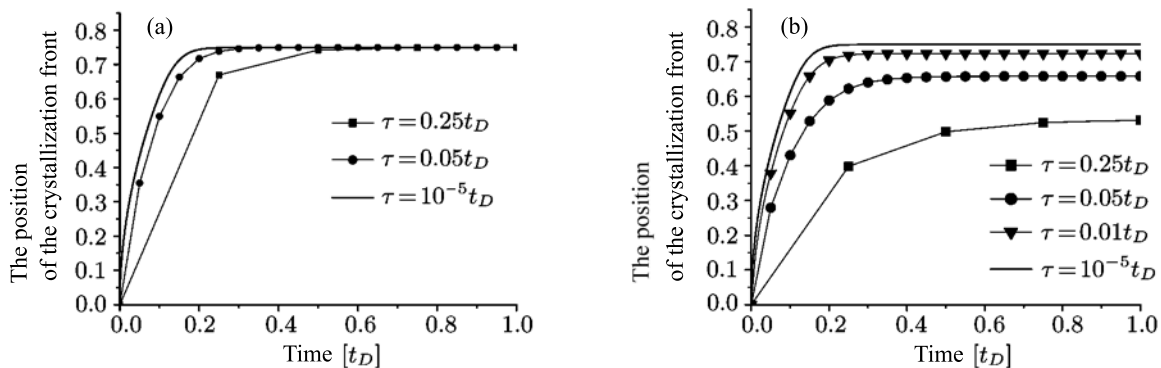


Fig. 2. The position of the crystallization front: (a) computations by scheme I; (b) computations by scheme II.

Results of computations by the scheme II

The increment τ	0.25	0.05	0.01	0.001	0.0001	0.00001
The layer width	0.534486	0.657992	0.723689	0.746612	0.749602	0.749957

Systems of nonlinear grid equations corresponding to schemes I and II are solved by the Newton method for the vector of unknowns whose components are the concentration at all grid nodes and the interface motion velocity. The linear equations on each iteration of the Newton method are solved by a special modification of the Thomas method [27].

Figure 2 (a) presents the dependence of the position of the crystallization front on time. In the figure, one can see that scheme I provides an almost exact value of the width of the grown solid phase even in the case of large time increments. Obviously, the time of exit of the grid solution to the stationary mode depends on the increment τ . Computations with a very fine time increment ($\tau = 10^{-5}t_D$) give the time $t_{st} = 0.575t_D$ of exit to the stationary mode. If $\tau = 0.25t_D$, then, by time t_{st} , the width $d(t)$ of the grown crystal is 99% Δ , $d(t_{st}) = 0.749925$. The computations with increment $\tau = 0.05$ also provide a good description of the initial stage of the process, $d(t_{st}) = 99.999\%\Delta$.

In the computations by scheme II with increment $\tau = 0.25$, the width of the grown layer on the stationary mode $t = 2.5t_D$ is 71.25% Δ . Therefore, the system has lost approximately 21% of the substance originally soluted in the liquid phase. The mass loss due to the presence of fictitious drains in the discrete model decreases with the time increment. Figure 2 (b) illustrates this assertion. The table presents the values of the layer width obtained in computations by scheme II for various τ . These data show that the accuracy provided by scheme I for $\tau_0 = 0.05$ is provided by scheme II for the time increment $\tau_0/5000$.

The results of computations visually illustrate the mechanism of action of the fictitious sources/drains appearing in the discrete medium owing to the failure of the principle of conservation. The considered process of crystallization of a binary solution is a relatively simple example of a thermodiffusion Stefan problem in which one can directly check how the mass conservation law is satisfied and adjust the time increment in the case of nonconservative systems. In multicomponent systems with complicated phase diagram where the process occurs in nonisothermal conditions, a failure of the energy and mass balance may result in a difficult-to-control shift of the phase equilibrium point along the phase diagram surface and to unpredictable results.

Therefore, for the thermodiffusion Stefan problem, we have constructed a family of conservative finite difference schemes that inherit the main properties of the original differential problem. We have singled out a class of finite difference schemes for which the front rectification method and the moving grid method are algebraically equivalent. In the present paper, we give the results of computations illustrating the action of fictitious sources appearing in the computations when using nonconservative schemes.

ACKNOWLEDGMENTS

The research was supported by the Program for Support of Leading Scientific Schools (project no. NSh-1434.2012.2), Program no. 15 of the Presidium of the Russian Academy of Sciences, and the Russian Foundation for Basic Research (project no. 12-01-00606).

REFERENCES

1. Tikhonov, A.N. and Samarskii, A.A., Convergence of Finite Difference Schemes in the Class of Discontinuous Coefficients, *Dokl. Akad. Nauk SSSR*, 1959, vol. 124, no. 3, pp. 1529–1532.
2. Tikhonov, A.N. and Samarskii, A.A., Homogeneous Finite Difference Schemes, *Zh. Vychisl. Mat. Mat. Fiz.*, 1961, vol. 1, no. 1, pp. 5–63.
3. Samarskii, A.A. and Popov, Yu.P., *Raznostnye metody resheniya zadach gazovoi dinamiki* (Finite Difference Methods for the Solution of Problems of Gas Dynamics), Moscow: Nauka, 1992.
4. Illingworth, T.C. and Golosnoy, I.O., Numerical Solutions of Diffusion-Controlled Moving Boundary Problems Which Conserve Solute, *J. Comput. Phys.*, 2005, vol. 209, pp. 207–225.

5. Muray, W.D. and Landis, F., Numerical and Machine Solutions of the Transient Heat Conduction Problems Involving Melting or Freezing, *J. Heat Transfer*, 1959, vol. 81, pp. 106–112.
6. Kutluay, S., Numerical Schemes for One-Dimensional Stefan-Like Problems with a Forcing Term, *Appl. Math. Comput.*, 2005, vol. 168, pp. 1159–1168.
7. Caldwell, J. and Kwan, Y-Y., A Brief Review of Several Numerical Methods for One-Dimensional Stefan Problems, *Thermal Sci.*, 2009, vol. 13, no. 2, pp. 61–72.
8. Savovic, S. and Caldwell, J., Numerical Solution of Stefan Problem with Time-Dependent Boundary Conditions by Variable Space Grid Method, *Thermal Sci.*, 2009, vol. 13, no. 4, pp. 165–174.
9. Crank, J., *Free and Moving Boundary Problems*, Oxford, 1987.
10. Samarskii, A.A. and Vabishchevich, P.N., *Vychislitel'naya teploperedacha* (Computational Heat Transfer), Moscow, 2003.
11. Samarskii, A.A. and Moiseenko, B.D., An Efficient Scheme for Shock-Capturing Computation in a Multidimensional Stefan Problem, *Zh. Vychisl. Mat. Mat. Fiz.*, 1965, vol. 5, no. 5, pp. 816–827.
12. Tikhonov, A.N. and Samarskii, A.A., *Upravleniya matematicheskoi fiziki* (Equations of Mathematical Physics), Moscow: Nauka, 1966.
13. Bakirova, O.I., Numerical Modeling of Processes of Zone Melting on the Basis of the Solution of the Problem on the Phase Transition in a Binary System, in *Mat. modelirovanie. Poluchenie monokristallov i poluprovodnikovyykh struktur* (Mathematical Modeling. Obtaining Monocrystals and Semiconducting Structures), Moscow, 1986, pp. 142–158.
14. Degtyarev, L.M., Drozdov, V.V., and Ivanova, T.S., The Method of Nets Adapted to the Solution in Singularly Perturbed One-Dimensional Boundary Value Problems, *Differ. Uravn.*, 1987, vol. 23, no. 7, pp. 1160–1168.
15. Vermolen, F.J. and Vuik, C., A Mathematical Model for the Dissolution of Particles in Multi-Component Alloys, *J. Comput. Appl. Math.*, 2000, vol. 126, pp. 233–254.
16. Friazinov, I.V., Marchenko, M.P., and Mazhorova, O.S., Transient Simulation of Crystal Growth by Bridgman Technique under Normal and Low Gravity, *Proceedings of Microgravity Science and Low Gravity. August 1991. Aerospace Congress*, Moscow, 1991, pp. 179–187.
17. Zhou, Yu. and North, T.H., Kinetic Modeling of Diffusion-Controlled, Two-Phase Moving Interface Problems, *Model. Simul. Material Sci. Eng.*, 1993, vol. 1, no. 4, pp. 505–516.
18. Pandelaers, L., Verhaeghe, F., Wollants, P., and Blanpain, B., An Implicit Conservative Scheme for Coupled Heat and Mass Transfer Problems with Multiple Moving Interfaces, *Internat. J. Heat Mass Transfer*, 2011, vol. 54, no. 5–6, pp. 1039–1045.
19. Mazhorova, O.S., Popov, Yu.P., and Shcheritsa, O.V., An Algorithm for Computing a Phase Transition in Multicomponent System, *Differ. Uravn.*, 2004, vol. 40, no. 7, pp. 1051–1060.
20. Mazhorova, O.S., Popov, Yu.P., and Shcheritsa, O.V., The Method of the Numerical Solution of Crystallization Problems for Multicomponent Solutions, *Preprint Inst. Appl. Math.*, Moscow, 2002, no. 18.
21. Landau, H.G., Heat Conduction in a Melting Solid, *J. Appl. Math.*, 1950, vol. 8, pp. 81–94.
22. Ufimtsev, V.B. and Akchurin, R.Kh., *Fiziko-khimicheskie osnovy zhidkofazovoi epitaksii* (Physical-Chemical Foundations of Liquid-Phase Epitaxy), Moscow, 1983.
23. Samarskii, A.A., *Vvedenie v teoriyu raznostnykh skhem* (Introduction to the Theory of Finite Difference Schemes), Moscow: Nauka, 1971.
24. Vermolen, F.J. and Vuik, C., A Numerical Method to Compute the Dissolution of Second Phases in Ternary Alloys, *J. Comput. Appl. Math.*, 1998, vol. 93, pp. 123–143.
25. Vitek, J.M., Vitek, S.A., and David, S.A., Numerical Modeling of Diffusion-Controlled Phase Transformation in Ternary Systems and Application to the Ferrite/Austenite Transformation in Fe-Cr-Ni System, *Metallurg. Mater. Trans. A*, 1995, vol. 26, pp. 2007–2025.
26. http://www.crct.polymtl.ca/fact/documentation/SGTE/SGTE_Figs.htm
27. Chcheritsa, O.V., Mazhorova, O.S., and Popov, Yu.P., Implicit Numerical Algorithm for the Solution of Phase Transition Problems in Multi-Component Alloys, *J. Math. Model. Anal.*, 2004, vol. 9, no. 4, pp. 253–266.

Reproduced with permission of the copyright owner. Further reproduction prohibited without permission.